Available online at www.sciencedirect.com
ScienceDirect
Acta Materialia 58 (2010) 5848–5857
Acta MATERIALIA
www.elsevier.com/locate/actamat

Lattice correspondence during twinning in hexagonal close-packed crystals

M. Niewczas *

Department of Materials Science and Engineering, McMaster University, Hamilton, Ontario, Canada L8S 4M1

Received 3 June 2010; received in revised form 28 June 2010; accepted 30 June 2010
Available online 3 August 2010

Abstract

The correspondence of the dominant slip modes in parent and twin structures in hexagonal closed-packed crystals is considered within the framework of the theory of deformation twinning. The correspondence matrices, which provide a link between the parent and twin lattices, have been worked out for compound twinning modes and selected metals. Geometrical considerations suggest that in most cases deformation twins should inherit a harder dislocation substructure than that of the corresponding parent. Possible mechanisms of twin hardening are discussed.
© 2010 Acta Materialia Inc. Published by Elsevier Ltd. All rights reserved.

Keywords: Hexagonal close-packed metals; Twinning; Lattice correspondence; Slip systems; Lattice transformation

1. Introduction

Hexagonal closed-packed (hcp) metals and alloys deform by slip and twinning, but due to a limited number of slip modes imposed by the hcp lattice, twinning becomes an important mechanism of plastic deformation in these structures. The role of twinning in the deformation of hcp materials has been the focus of intensive theoretical and experimental studies (for a review of the relevant literature see Ref. [1]). These studies rely heavily on understanding the crystallographic nature of twinning and its influence on the material microstructure.

When twinning occurs, the parent crystal is sheared to a new orientation determined by the operating twinning mode. The crystallographic relationship between parent and twin is described uniquely by the correspondence matrix: each vector or plane in the parent lattice is related unambiguously to a corresponding vector or plane in the twinned lattice [2]. This lattice correspondence is a key concept in the theory of deformation twinning by Bevis and Crocker [3].

The correspondence matrix method was used to study crystallographic relationships during mechanical twinning in face-centered cubic (fcc) crystals [4], supertwinning in fcc and body-centered cubic (bcc) crystals [5] and to investigate the nature of lattice defects inherited by twins in fcc crystals [4,6,7], gamma-TiAl [8] and more recently in Zr [9].

The present work is concerned with analysis of the lattice correspondence between parent and twin developed as a result of different twining modes in hcp metals having different c/a ratios. Section 2 of this paper outlines the basic crystallography of mechanical twinning in the hcp crystal system. Section 3 examines the correspondence matrix method, which provides a convenient framework for analysis of the transformation of crystallographic planes and directions. The last section, Section 4, follows the analysis of the correspondence between slip modes in parent and twin lattices of Mg and Zr. The results are relevant to studies of the lattice transformations in cubic and non-cubic materials, transmission electron microscopy (TEM) studies of deformed hcp materials and analysis of their diffraction patterns, analysis of lattice defects

* Tel.: +1 905 525 9140x23498; fax: +1 905 521 2773.
E-mail address: niewczas@mcmaster.ca

1359-6454/$36.00 © 2010 Acta Materialia Inc. Published by Elsevier Ltd. All rights reserved.
doi:10.1016/j.actamat.2010.06.059

produced by twinning, analysis of twin–twin intersections and double twining processes, and in modeling plastic deformation and mechanical properties of cubic and non-cubic systems undergoing mechanical twinning.

2. Crystallography of deformation twinning in hcp crystals

For a comprehensive treatment of the crystallography of deformation twining in various crystal systems the reader is referred to the textbooks of Christian [2], Kelly and Groves [10], papers of Bevis and Crocker [3,11] and Partridge [12] and more recent work of Christian and Mahajan [13]. Here we briefly review the basic crystallography of mechanical twinning pertinent to the present work.

On the microscopic scale, deformation twinning is accomplished by coordinated displacements of atoms along well-defined crystallographic directions on well-defined crystallographic planes, resulting in homogeneous shearing of the crystal lattice and formation of a new lattice in twin orientation to the parent lattice. Fig. 1 shows a well-known diagrammatic representation of a twinning shear distorting a sphere (parent lattice) into an ellipsoid (twin lattice) in a projection onto the so-called plane of shear, S. The crystallographic relationship between these two lattices is described by four interdependent twinning elements K_1, K_2, η_1, and η_2 [2,14]. The twinning shear occurs in the K_1 plane along the η_1 direction. The K_1 plane, the invariant plane, preserves its crystallographic identity in the twin lattice. The conjugate to the twinning plane is K_2; it rotates to

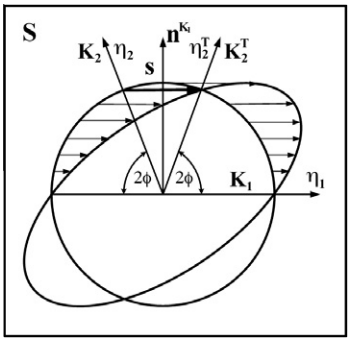

Fig. 1. Distortion of a sphere into an ellipsoid during twinning shear s along the η_1 direction in K_1 plane. n^{K1} is normal to K_1 plane. K_2 is the conjugate to the twinning plane with η_2 direction enclosed in the plane. K_2 rotates to K_2^T, η_2 to η_2^T direction. The section is parallel to the plane of shear S. Magnitude of shear $s = 2\cot 2\phi$ [2].

K_2^T in the twin, and it also conserves its type in the twin lattice. The K_2 plane contains the η_2 direction, defined as the conjugate twinning direction or conjugate shear direction; it rotates during twinning to η_2^T in the K_2^T plane in the twin. Another important plane is S, the plane of the shear, the projection plane in Fig. 1. The S plane is extended on η_1, and η_2 or alternatively defined as the plane containing η_1, and the normals to the K_1 and K_2 planes. When twinning occurs, the material above the K_1 plane is sheared by an amount defined by the twinning shear, s. The magnitude of the twinning shear determines the position of the K_2^T plane and η_1^T in the twin lattice. In the hcp lattice the twining shear s depends on the c/a ratio. The magnitude of the shear is related to an angle, 2ϕ, between K_1 and K_2 or equivalently K_2^T and K_1, such that $s = 2\cot 2\phi$ (Fig. 1). A twinning mode is uniquely specified by either K_1 and η_2 or K_2 and η_1.

Deformation twins for which parent and twin lattices are related by reflection in the K_1 plane fall into two categories: Type I, for which the twin lattice results from rotation by 180° around the normal to the K_1 plane; and Type II, where the rotation is about η_1. In contrast to the situation in fcc and bcc crystals where K_1 and K_2 and η_1 and η_2 are rational, the twinning elements in hcp material may represent irrational planes and directions [3,13]. In this work we focus on Type I twins for which all four twinning elements K_1, K_2, η_1, and η_2 are rational; these are known as compound twins.

Table 1 shows twinning parameters of four twinning modes considered in this work [15]. $\{1\ 0\ \bar{1}\ 2\} \pm \langle 1\ 0\ \bar{1}\ \bar{1}\rangle$ is a twinning mode observed during compression deformation in Cd and Zn and tensile deformation in Co, Mg, Zr, Ti, Be and many alloys of these elements. $\{1\ 0\ \bar{1}\ 1\}$ $\langle 1\ 0\ \bar{1}\ \bar{2}\rangle$ represents a compressive twinning mode common in Mg and occasionally also reported in Ti. $\{1\ 1\ \bar{2}\ 1\}$ $\langle \bar{1}\ \bar{1}\ 2\ 6\rangle$ is twinning, which occurs frequently during tensile deformation of Co, Re, Zr and observed also in Ti and graphite. $\{1\ 1\ \bar{2}\ 2\}\langle 1\ 1\ \bar{2}\ \bar{3}\rangle$ represents compressive twinning observed frequently in Ti, Zr and their alloys [16]. Fig. 2 shows a perspective view of the twinning modes discussed throughout this work.

3. Parent–twin lattice correspondence

The purpose of this section is to develop for hcp crystals a general expression, which describes an arbitrary lattice vector before and after twinning. This relationship is

Table 1
Crystallographic elements of compound twins in hcp crystals (γ represents c/a ratio for a given metal) [15].

K_1	K_2	η_1	η_2	Shear plane	Shear	Material
$\{10\bar{1}2\}$	$\{10\bar{1}\bar{2}\}$	$\pm\langle 10\bar{1}\bar{1}\rangle$	$\langle 10\bar{1}1\rangle$	$\{1\bar{2}10\}$	$\frac{\lvert\gamma^2-3\rvert}{\gamma\sqrt{3}}$	Cd, Zn, Co, Mg, Zr, Ti, Be
$\{10\bar{1}1\}$	$\{10\bar{1}\bar{3}\}$	$\langle 10\bar{1}\bar{2}\rangle$	$\langle 30\bar{3}2\rangle$	$\{1\bar{2}10\}$	$\frac{4\gamma^2-9}{4\gamma\sqrt{3}}$	Mg, Ti
$\{11\bar{2}2\}$	$\{11\bar{2}\bar{4}\}$	$\frac{1}{3}\langle 11\bar{2}\bar{3}\rangle$	$\frac{1}{3}\langle 22\bar{4}3\rangle$	$\{1\bar{1}00\}$	$\frac{2(\gamma^2-2)}{3\gamma}$	Ti, Zr
$\{11\bar{2}1\}$	(0002)	$\frac{1}{3}\langle \bar{1}\bar{1}26\rangle$	$\frac{1}{3}\langle 1120\rangle$	$\{\bar{1}100\}$	$\frac{1}{\gamma}$	Co, Re, Zr, Ti, graphite

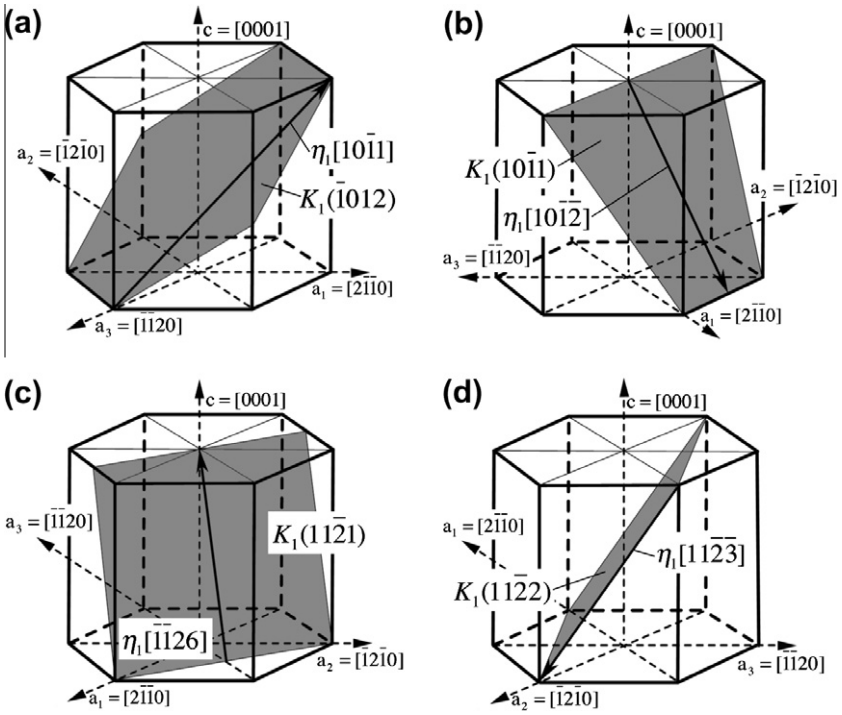

Fig. 2. Perspective view on the twinning modes considered in this work. (a) $(\bar{1}\ 0\ 1\ 2)[1\ 0\ \bar{1}\ 1]$ tensile twinning mode characteristic for Co, Mg, Zr, Ti and Be. Opposite sense of the shear to this shown in the figure, would represent compressive twinning mode in Cd and Zn. (b) $(1\ 0\ \bar{1}\ 1)[1\ 0\ \bar{1}\ \bar{2}]$ compressive twinning mode occurring in Mg. (c) $(1\ 1\ \bar{2}\ 1)[\bar{1}\ \bar{1}\ 2\ 6]$ tensile twinning mode characteristic for Co, Re and Zr. (d) $(1\ 1\ \bar{2}\ 2)[1\ 1\ \bar{2}\ \bar{3}]$ compressive twinning observed in Ti and Zr.

defined uniquely by the correspondence matrix. The following is devoted to derivation of the correspondence matrix for different twinning modes in the hcp crystal structure.

For numerical computations involving the hcp lattice, it is convenient to express the four-index Miller–Bravais indices of crystallographic planes and directions in terms of a three-index orthogonal coordinate system and to carry out all computations in terms of the orthogonal system. The general procedure for calculating correspondence relations between parent and twin in an hcp lattice thus involves transformation of crystallographic planes and directions to an orthogonal system, performing the desired computations, and re-indexing into hexagonal indices.

The transformation equations between hexagonal and orthogonal notation and the reverse transformations are given in Appendix A. In the subsequent part of this section the crystallographic planes and directions of the hcp lattice are expressed in terms of the orthogonal notation. The correspondence relations between the parent and twin lattices can be derived by a procedure described elsewhere for cubic lattices [6].

Type I twinning shear is accomplished by the homogeneous deformation of a crystal lattice described by a deformation gradient tensor in the form [17]:

$$\mathbf{S} = \begin{bmatrix} 1 + sm_1n_1 & sm_1n_2 & sm_1n_3 \\ sm_2n_1 & 1 + sm_2n_2 & sm_2n_3 \\ sm_3n_1 & sm_3n_2 & 1 + sm_3n_3 \end{bmatrix} \tag{1}$$

where s is the magnitude of the twinning shear, $m = [m_1, m_2, m_3]$ the twinning direction, and $n = [n_1, n_2, n_3]$ is the normal to the twinning plane K_1. During twinning shear the volume of the material is unchanged and the determinant of the deformation gradient matrix $\mathbf{S}$ is 1.

Any vector $\mathbf{u_M} = [u_1, u_2, u_3]$ defined with respect to the orthogonal system in the parent lattice is sheared to the vector $\mathbf{v_M} = [v_1, v_2, v_3]$ in the same lattice, according to the linear transformation relation:

$$\mathbf{v_M} = \mathbf{S}\ \mathbf{u_M} \tag{2}$$

where $\mathbf{u_M}$ and $\mathbf{v_M}$ denote column vectors and $\mathbf{S}$ is a 3×3 matrix built from the components of the second rank deformation tensor, all expressed with reference to the parent axis system. The transformation given by Eq. (2) is affine, i.e., after deformation collinear points remain collinear and coplanar lines remain coplanar. The peculiar feature of the twinning shear applied to the vector $\mathbf{u_M}$ is that the sheared product vector, $\mathbf{v_M}$, is located in the new twin lattice, defined by the new basis system.

The following transformation is used to express $\mathbf{v_M}$ in terms of the basis system of the twin:

$$\mathbf{v_T} = \mathbf{X}^{-1}\ \mathbf{R}\ \mathbf{X}\ \mathbf{v_M} \tag{3}$$

where $\mathbf{v_T}$ is a vector defined with reference to the basis axis system in the twin lattice, $\mathbf{X}$ is the transformation matrix between parent and the coordinate system associated with the matrix–twin interface and $\mathbf{R}$ is rotation matrix describing rotation of the parent lattice around the normal to the

twinning plane. For Type I twinning the **X** and **R** matrices have the following form [2,6]:

$$\mathbf{X} = \begin{bmatrix} m_1 & m_2 & m_3 \\ m_3n_2 - m_2n_3 & m_1n_3 - m_3n_1 & m_2n_1 - m_1n_2 \\ n_1 & n_2 & n_3 \end{bmatrix} \tag{4}$$

$$\mathbf{R} = \begin{bmatrix} -1 & 0 & 0 \\ 0 & -1 & 0 \\ 0 & 0 & 1 \end{bmatrix} \tag{5}$$

The product of matrix multiplication $\mathbf{X}^{-1}\,\mathbf{R}\,\mathbf{X}$ we denote as the re-indexation matrix **U**. In this formulation the re-indexation matrix $\mathbf{U} = \mathbf{X}^{-1}\,\mathbf{R}\,\mathbf{X}$ is obtained as an orthogonal similarity transformation of the operator matrix **R**, which rotates the parent lattice 180° around the normal to the K_1 plane. The above procedure requires introduction of the coordinate system associated with the parent–twin interface to construct matrix **X** in Eq. (4). In this coordinate system, the first axis is parallel to the twinning shear direction m, the third axis coincides with the normal to the K_1 plane, the second axis is the cross product of these two [2,6].

The re-indexation matrix can also be devised from a general form of a three-dimensional rotation matrix around arbitrary direction $q = [q_1, q_2, q_3]$ and arbitrary angle θ, given by:

$$\mathbf{R}^{3D} = \begin{bmatrix} q_1^2(1-\cos\theta) + \cos\theta & q_1q_2(1-\cos\theta) - q_3\sin\theta & q_1q_3(1-\cos\theta) + q_2\sin\theta \\ q_1q_2(1-\cos\theta) + q_3\sin\theta & q_2^2(1-\cos\theta) + \cos\theta & q_2q_3(1-\cos\theta) - q_1\sin\theta \\ q_1q_3(1-\cos\theta) - q_2\sin\theta & q_2q_3(1-\cos\theta) + q_1\sin\theta & q_3^2(1-\cos\theta) + \cos\theta \end{bmatrix} \tag{6}$$

In our case the rotation axis $q = [q_1, q_2, q_3]$ is the normal to the K_1 plane and θ, the rotation angle of a parent lattice around q required to obtain a twin lattice, is 180°. In this formulation the re-indexation matrix reads:

$$\mathbf{U} = \begin{bmatrix} -1 + 2q_1^2 & 2q_1q_2 & 2q_1q_3 \\ 2q_1q_2 & -1 + 2q_2^2 & 2q_2q_3 \\ 2q_1q_3 & 2q_2q_3 & -1 + 2q_3^2 \end{bmatrix} \tag{7}$$

The re-indexation matrix allows any vector or plane in the parent lattice to be expressed as its corresponding representation in the twin lattice. Thus, components of arbitrary vector $\mathbf{b_M}$ or arbitrary plane $\mathbf{n_M}$ of the parent, are expressed in the twin lattice by means of the re-indexation transformation such that:

$$\mathbf{b_T} = \mathbf{U}\,\mathbf{b_M} \tag{8}$$

and

$$\mathbf{n_T} = \mathbf{n_M}\,\mathbf{U}^{-1} \tag{9}$$

$\mathbf{b_T}$ and $\mathbf{b_M}$ are column vectors, whereas $\mathbf{n_T}$ and $\mathbf{n_M}$ are row vectors.

The indexation of a vector or a plane with respect to either matrix or twin coordinates described by Eqs. (8) and (9) is an important concept in lattice correspondence. A twinning mode is identified by examining misorientation of the related directions or planes in two lattices. For example, $(\bar{1}\ 0\ 1\ 2)[1\ 0\ \bar{1}\ 1]$ twinning mode in Mg is recognized from the ~86° missorientation between parent and twin. The exact angle 86.31°, is obtained by considering the angle between c-axis in the parent and c-axis in the twin, i.e., the angle between [0001] and its associate vector $[\overline{29}\ 0\ 29\ 2]$. The latter vector being $[0001]_M$ re-indexed in the twin lattice by means of Eq. (8) and the re-indexation matrix for the $(\bar{1}\ 0\ 1\ 2)[1\ 0\ \bar{1}\ 1]$ twining mode, i.e., $[0001]_M = [\overline{29}\ 0\ 29\ 2]_T$ (Table 2a, Appendix B).

Comparing Eqs. (2) and (3) it is evident that vector $\mathbf{u_M}$ is related to the vector $\mathbf{v_T}$ by:

$$\mathbf{v_T} = \mathbf{X}^{-1}\,\mathbf{R}\,\mathbf{X}\,\mathbf{S}\,\mathbf{u_M} \tag{10}$$

Thus,

$$\mathbf{v_T} = \mathbf{U}\,\mathbf{S}\,\mathbf{u_M} \tag{11}$$

The above equation incorporates the effect both of deformation of the vector $\mathbf{u_M}$ and the change of coordinate system. After replacing matrix product **U S** by the matrix **C**, the correspondence matrix, Eq. (11) can be rewritten:

$$\mathbf{v_T} = \mathbf{C}\,\mathbf{u_M} \tag{12}$$

It is now evident that vector $\mathbf{v_T}$ in the twinned lattice is directly related to the original vector $\mathbf{u_M}$ in the parent crystal through the correspondence matrix, **C**, and the linear transformation relation (12). Similarly, any crystallographic plane $\mathbf{n_M}$ in the parent lattice is related to a plane $\mathbf{n_T}$, in the twinned lattice according to relation (13):

$$\mathbf{n_T} = \mathbf{n_M}\,\mathbf{C}^{-1} \tag{13}$$

as before, $\mathbf{v_T}$ and $\mathbf{u_M}$ are column vectors and $\mathbf{n_T}$ and $\mathbf{n_M}$ are row vectors.

Deformation, re-indexation and correspondence matrices are all unimodular, i.e., their determinant is unity. This means that a shear, a rotation, or a shear followed by rotation, produced by operation of these matrices on the crystal lattice, preserves the crystal volume. For conventional twinning modes associated with the rational twinning elements, the correspondence matrix is equal to its inverse [3,13].

Tables 2a–2d provide explicit forms of deformation, re-indexation, and correspondence matrices for different twinning modes in Cd, Mg, Zr, Ti and Be. One can verify that in all cases considered, the correspondence matrix is equal to the inverse of the correspondence matrix, i.e., $\mathbf{C} = \mathbf{C}^{-1}$. Also, the trace of every matrix **C** in Table 2, is equal to −1 ($\mathrm{tr}\,\mathbf{C} = -1$), indicating that these matrices represent deformation twining of a classical type [3,11,13,14].

Table 2a
Deformation **S**, re-indexation **U** and correspondence **C** matrices for different twinning modes of Cd with $c/a = 1.886$.

K_1/η_1	Magnitude of shear s	Deformation matrix **S**	Re-indexation matrix **U**	Correspondence matrix **C**
$(\bar{1}012)$ $[10\bar{1}1]$	0.17051	$\begin{bmatrix} 0.93629 & -0.0367831 & 0.0675611 \\ -0.0367831 & 0.978763 & 0.0390064 \\ -0.0801049 & -0.0462486 & 1.08495 \end{bmatrix}$	$\begin{bmatrix} -0.18629 & 0.469796 & -0.862895 \\ 0.469796 & -0.728763 & -0.498193 \\ -0.862895 & -0.498193 & -0.0849468 \end{bmatrix}$	$\begin{bmatrix} -0.12258 & 0.506579 & -0.930456 \\ 0.506579 & -0.707527 & -0.537199 \\ -0.78279 & -0.451944 & -0.169894 \end{bmatrix}$
$(10\bar{1}1)$ $[10\bar{1}\bar{2}]$	0.400103	$\begin{bmatrix} 1.1138 & 0.0657008 & 0.0603378 \\ 0.0657008 & 1.03793 & 0.034836 \\ -0.286162 & -0.165216 & 0.848271 \end{bmatrix}$	$\begin{bmatrix} 0.238797 & 0.71522 & 0.656838 \\ 0.71522 & -0.587068 & 0.379226 \\ 0.656838 & 0.379226 & -0.651729 \end{bmatrix}$	$\begin{bmatrix} 0.125 & 0.649519 & 0.596501 \\ 0.649519 & -0.625 & 0.34439 \\ 0.943 & 0.544441 & -0.5 \end{bmatrix}$
$(11\bar{2}2)$ $[11\bar{2}\bar{3}]$	0.55037	$\begin{bmatrix} 1.05695 & 0.0986321 & 0.0603873 \\ 0.0986321 & 1.17084 & 0.104594 \\ -0.214798 & -0.37204 & 0.772219 \end{bmatrix}$	$\begin{bmatrix} -0.609721 & 0.675982 & 0.413869 \\ 0.675982 & 0.170836 & 0.716842 \\ 0.413869 & 0.716842 & -0.561114 \end{bmatrix}$	$\begin{bmatrix} -0.666667 & 0.57735 & 0.353482 \\ 0.57735 & 0 & 0.612248 \\ 0.628667 & 1.08888 & -0.333333 \end{bmatrix}$
$(11\bar{2}1)$ $[\bar{1}\bar{1}26]$	0.530223	$\begin{bmatrix} 0.967166 & -0.0568707 & -0.0174095 \\ -0.0568707 & 0.901497 & -0.0301541 \\ 0.247702 & 0.429032 & 1.13134 \end{bmatrix}$	$\begin{bmatrix} -0.532834 & 0.809155 & 0.247702 \\ 0.809155 & 0.401497 & 0.429032 \\ 0.247702 & 0.429032 & -0.868663 \end{bmatrix}$	$\begin{bmatrix} -0.5 & 0.866025 & 0.265111 \\ 0.866025 & 0.5 & 0.459186 \\ 0.0 & 0.0 & -1.0 \end{bmatrix}$

Table 2b
Deformation **S**, re-indexation **U** and correspondence **C** matrices for different twinning modes of Mg with $c/a = 1.624$.

K_1/η_1	Magnitude of shear s	Deformation matrix **S**	Re-indexation matrix **U**	Correspondence matrix **C**
$(\bar{1}012)$ $[10\bar{1}1]$	0.128917	$\begin{bmatrix} 0.951756 & -0.0278535 & 0.0594135 \\ -0.0278535 & 0.983919 & 0.0343024 \\ -0.0522319 & -0.0301561 & 1.06432 \end{bmatrix}$	$\begin{bmatrix} -0.298244 & 0.405159 & -0.864232 \\ 0.405159 & -0.766081 & -0.498965 \\ -0.864232 & -0.498965 & 0.064325 \end{bmatrix}$	$\begin{bmatrix} -0.25 & 0.433013 & -0.923645 \\ 0.433013 & -0.75 & -0.533267 \\ -0.812 & -0.468808 & 0 \end{bmatrix}$
$(10\bar{1}1)$ $[10\bar{1}\bar{2}]$	0.137717	$\begin{bmatrix} 1.04288 & 0.0247594 & 0.0264067 \\ 0.0247594 & 1.01429 & 0.0152459 \\ -0.0928593 & -0.0536123 & 0.942821 \end{bmatrix}$	$\begin{bmatrix} 0.167885 & 0.674278 & 0.719141 \\ 0.674278 & -0.610705 & 0.415196 \\ 0.719141 & 0.415196 & -0.557179 \end{bmatrix}$	$\begin{bmatrix} 0.125 & 0.649519 & 0.692734 \\ 0.649519 & -0.625 & 0.39995 \\ 0.812 & 0.468808 & -0.5 \end{bmatrix}$
$(11\bar{2}2)$ $[11\bar{2}\bar{3}]$	0.261649	$\begin{bmatrix} 1.0292 & 0.0505844 & 0.0359667 \\ 0.0505844 & 1.08761 & 0.0622961 \\ -0.0948576 & -0.164298 & 0.8831 \end{bmatrix}$	$\begin{bmatrix} -0.637462 & 0.627935 & 0.446476 \\ 0.627935 & 0.0876148 & 0.773319 \\ 0.446476 & 0.773319 & -0.450153 \end{bmatrix}$	$\begin{bmatrix} -0.666667 & 0.57735 & 0.410509 \\ 0.57735 & 0 & 0.711022 \\ 0.541333 & 0.937617 & -0.333333 \end{bmatrix}$
$(11\bar{2}1)$ $[\bar{1}\bar{1}26]$	0.615764	$\begin{bmatrix} 0.956708 & -0.0749838 & -0.0266576 \\ -0.0749838 & 0.870124 & -0.0461723 \\ 0.281224 & 0.487095 & 1.17317 \end{bmatrix}$	$\begin{bmatrix} -0.543292 & 0.791042 & 0.281224 \\ 0.791042 & 0.370124 & 0.487095 \\ 0.281224 & 0.487095 & -0.826832 \end{bmatrix}$	$\begin{bmatrix} -0.5 & 0.866025 & 0.307882 \\ 0.866025 & 0.5 & 0.533267 \\ 0.0 & 0.0 & -1.0 \end{bmatrix}$

The correspondence matrix method summarized by Eqs. (12) and (13) represents an essential tool in predicting the physical transformation of crystallographic directions and planes resulting from twinning. The correspondence matrix approach is indispensable in applications such as analysis of the nature of defects inherited by deformation twinning [4,6,7], analysis of interactions between slip dislocations and twin boundaries, in problems of incorporating a glide dislocations in the parent into the twin lattice through the matrix–twin interface, and in problems related to twin–twin intersections and double twinning processes. To the best of the author's knowledge most continuum-based approaches for modeling plastic deformation of crystalline materials currently available (for review of the subject and the literature available there see Ref. [18]) treat mechanical twinning incorrectly. They rely solely on rotation principles in indexing planes and directions inside the mechanical twins and therefore miss an important part of the processes coupled to the lattice transformation. In the next section, the method described here is used to examine the correspondence relations of dominant slip modes in hcp crystals.

4. Correspondence of slip modes in Mg and Zr

It is useful to explore in some detail the relationship between slip modes in the parent and twin lattices of actual hcp metals and consider how the nature of dislocations incorporated to the twin may influence its hardening.

The hardening of deformation twin results from at least two independent mechanisms. One is the Hall–Petch effect associated with the twin size and the reduction in dislocation mean free path and the other arises from intrinsic strength of the twin substructure inherited from the parent. The latter effect is difficult to evaluate by the methods employed here but it may occur through various processes including: the increase of the length of the Burgers vector of transformed dislocations [4], decrease of the mobility of dislocations, formation of sessile dislocations and three-dimensional defects of sessile character, formation of extended stacking faults and planar defects, formation of complex defects, other processes [6].

Tables 3 and 4 show the purely geometrical relation between planes and directions before and after twinning

Table 2c
Deformation **S**, re-indexation **U** and correspondence **C** matrices for different twinning modes Zr with $c/a = 1.594$.

K_1/η_1	Magnitude of shear s	Deformation matrix **S**	Re-indexation matrix **U**	Correspondence Matrix **C**
$(\bar{1}012)$ $[10\bar{1}1]$	0.16631	$\begin{bmatrix} 0.937848 & -0.0358834 & 0.0779822 \\ -0.0358834 & 0.979283 & 0.045023 \\ -0.0660467 & -0.0381321 & 1.08287 \end{bmatrix}$	$\begin{bmatrix} -0.312152 & 0.397129 & -0.863047 \\ 0.397129 & -0.770717 & -0.49828 \\ -0.863047 & -0.49828 & 0.0828691 \end{bmatrix}$	$\begin{bmatrix} -0.25 & 0.433013 & -0.941029 \\ 0.433013 & -0.75 & -0.543303 \\ -0.797 & -0.460148 & 0 \end{bmatrix}$
$(10\bar{1}1)$ $[10\bar{1}\bar{2}]$	0.105341	$\begin{bmatrix} 1.03314 & 0.0191343 & 0.0207915 \\ 0.0191343 & 1.01105 & 0.012004 \\ -0.0704369 & -0.0406668 & 0.955811 \end{bmatrix}$	$\begin{bmatrix} 0.158142 & 0.668653 & 0.726563 \\ 0.668653 & -0.613953 & 0.419481 \\ 0.726563 & 0.419481 & -0.544189 \end{bmatrix}$	$\begin{bmatrix} 0.125 & 0.649519 & 0.705772 \\ 0.649519 & -0.625 & 0.407477 \\ 0.797 & 0.460148 & -0.5 \end{bmatrix}$
$(11\bar{2}2)$ $[11\bar{2}\bar{3}]$	0.226197	$\begin{bmatrix} 1.02546 & 0.044093 & 0.0319411 \\ 0.044093 & 1.07637 & 0.0553237 \\ -0.0811572 & -0.140568 & 0.898172 \end{bmatrix}$	$\begin{bmatrix} -0.64121 & 0.621443 & 0.450176 \\ 0.621443 & 0.0763712 & 0.779728 \\ 0.450176 & 0.779728 & -0.435162 \end{bmatrix}$	$\begin{bmatrix} -0.666667 & 0.57735 & 0.418235 \\ 0.57735 & 0 & 0.724404 \\ 0.531333 & 0.920296 & -0.333333 \end{bmatrix}$
$(11\bar{2}1)$ $[\bar{1}\bar{1}26]$	0.627353	$\begin{bmatrix} 0.955211 & -0.0775776 & -0.0280988 \\ -0.0775776 & 0.865632 & -0.0486685 \\ 0.285578 & 0.494635 & 1.17916 \end{bmatrix}$	$\begin{bmatrix} -0.544789 & 0.788448 & 0.285578 \\ 0.788448 & 0.365632 & 0.494635 \\ 0.285578 & 0.494635 & -0.820842 \end{bmatrix}$	$\begin{bmatrix} -0.5 & 0.866025 & 0.313676 \\ 0.866025 & 0.5 & 0.543303 \\ 0.0 & 0.0 & -1.0 \end{bmatrix}$

Table 2d
Deformation **S**, re-indexation **U** and correspondence **C** matrices for different twinning modes in Ti with $c/a = 1.587$.

K_1/η_1	Magnitude of shear s	Deformation matrix **S**	Re-indexation matrix **U**	Correspondence matrix **C**
$(\bar{1}012)$ $[10\bar{1}1]$	0.175144	$\begin{bmatrix} 0.934571 & -0.0377753 & 0.0824559 \\ -0.0377753 & 0.97819 & 0.047606 \\ -0.0692237 & -0.0399663 & 1.08724 \end{bmatrix}$	$\begin{bmatrix} -0.315429 & 0.395237 & -0.862724 \\ 0.395237 & -0.77181 & -0.498094 \\ -0.862724 & -0.498094 & 0.0872384 \end{bmatrix}$	$\begin{bmatrix} -0.25 & 0.433013 & -0.94518 \\ 0.433013 & -0.75 & -0.5457 \\ -0.7935 & -0.458127 & 0.0 \end{bmatrix}$
$(10\bar{1}1)$ $[10\bar{1}\bar{2}]$	0.0977053	$\begin{bmatrix} 1.03081 & 0.0177897 & 0.0194157 \\ 0.0177897 & 1.01027 & 0.0112096 \\ -0.0651996 & -0.037643 & 0.958916 \end{bmatrix}$	$\begin{bmatrix} 0.155813 & 0.667309 & 0.7283 \\ 0.667309 & -0.614729 & 0.420484 \\ 0.7283 & 0.420484 & -0.541084 \end{bmatrix}$	$\begin{bmatrix} 0.125 & 0.649519 & 0.708885 \\ 0.649519 & -0.625 & 0.409275 \\ 0.7935 & 0.458127 & -0.5 \end{bmatrix}$
$(11\bar{2}2)$ $[11\bar{2}\bar{3}]$	0.21784	$\begin{bmatrix} 1.03397 & 0.0196137 & 0.0428127 \\ 0.058841 & 1.03397 & 0.0741538 \\ -0.107827 & -0.0622538 & 0.864112 \end{bmatrix}$	$\begin{bmatrix} -0.133894 & 0.500046 & 1.0915 \\ 0.62448 & -0.639456 & 0.786995 \\ 0.613654 & 0.354293 & -0.226649 \end{bmatrix}$	$\begin{bmatrix} -0.226713 & 0.446458 & 0.974527 \\ 0.52321 & -0.697925 & 0.659369 \\ 0.679787 & 0.392475 & -0.143306 \end{bmatrix}$
$(11\bar{2}1)$ $[\bar{1}\bar{1}26]$	0.63012	$\begin{bmatrix} 0.95485 & -0.0782015 & -0.0284497 \\ -0.0782015 & 0.864551 & -0.0492763 \\ 0.28661 & 0.496423 & 1.1806 \end{bmatrix}$	$\begin{bmatrix} -0.54515 & 0.787824 & 0.28661 \\ 0.787824 & 0.364551 & 0.496423 \\ 0.28661 & 0.496423 & -0.819401 \end{bmatrix}$	$\begin{bmatrix} -0.5 & 0.866025 & 0.31506 \\ 0.866025 & 0.5 & 0.5457 \\ 0.0 & 0.0 & -1.0 \end{bmatrix}$

for magnesium and zirconium respectively. For $(\bar{1}\ 0\ 1\ 2)$ $[1\ 0\ \bar{1}\ 1]$ tensile twinning in Mg the basal plane, $\{0001\}_M$, is transformed to a $\{1\ 0\ \bar{1}\ 0\}_T$ prism plane, while slip directions of the type $\langle 1\ 1\ \bar{2}\ 0\rangle_M$ are transformed to either $\langle 1\ 1\ \bar{2}\ 0\rangle_T$ or $\langle 1\ 1\ \bar{2}\ 3\rangle_T$ (Table 3a). If basal dislocations $\langle a\rangle$ follow the same geometry of transformation as a $\{0\ 0\ 0\ 1\}\langle 1\ 1\ \bar{2}\ 0\ \rangle$ slip system, i.e., if after passage of the twinning shear they are deposited onto a $\{1\ 0\ \bar{1}\ 0\}_T$ prism plane in the twin and acquire a new and longer Burgers vector, then they would be expected to be less mobile and a stronger obstacles in the twin lattice. A similar argument applies to the pyramidal $\langle a\rangle$ dislocations, the majority of the pyramidal $\langle c+a\rangle$ dislocations, and to prism dislocations with the exception of dislocations associated with the $(1\ 0\ \bar{1}\ 0)[\bar{1}\ 2\ \bar{1}\ 0]$ slip system, which transforms to $(0\ 0\ 0\ 1)[1\ \bar{2}\ 1\ 0]_T$. In the latter case the prism dislocations would assume a close-packed glide plane and an $\langle a\rangle$ Burgers vector and presumably would be more glissile in the twin than in the parent. These qualitative considerations suggest that the substructure of $(\bar{1}\ 0\ 1\ 2)[1\ 0\ \bar{1}\ 1]$ tensile twins in Mg should be harder than the corresponding parent substructure provided the latter contains dislocations from different slip systems.

Examination of the correspondence of slip systems for $(1\ 0\ \bar{1}\ 1)[1\ 0\ \bar{1}\ \bar{2}]$ compressive twinning in Mg suggest that a similar process occurs (Table 3b). With some exceptions, i.e., $(0\ 0\ 0\ 1)[\bar{1}\ 2\ \bar{1}\ 0]$ basal slip, $(1\ 0\ \bar{1}\ 1)[\bar{1}\ 2\ \bar{1}\ 0]$ and $(\bar{1}\ 0\ 1\ 1)[\bar{1}\ 2\ \bar{1}\ 0]$ pyramidal slip and $(1\ 0\ \bar{1}\ 1)[\bar{1}\ \bar{1}\ 2\ 3]$ and $(1\ 0\ \bar{1}\ 1)[\bar{2}\ 1\ 1\ 3]$ pyramidal $\langle c+a\rangle$ slip, the glide planes and glide directions are sheared to lower symmetry planes and directions, suggesting that dislocations associated with these slip systems should acquire lower mobility and presumably should strengthen the twin substructure.

Evidently, the same considerations apply to $(1\ 1\ \bar{2}\ 2)$ $[1\ 1\ \bar{2}\ \bar{3}]$ compression twinning in Zr (Table 4a) but not to $(1\ 1\ \bar{2}\ 1)[\bar{1}\ \bar{1}\ 2\ 6]$ tensile twining (Table 4b). In the latter case all basal and prismatic slip systems and the majority of pyramidal $\langle a\rangle$ and pyramidal $\langle c+a\rangle$ slip systems are unchanged by twinning transformation. Of six pyramidal $\langle a\rangle$ slip systems, four preserve their plane and direction in

Table 2e
Deformation **S**, re-indexation **U** and correspondence **C** matrices for different twinning modes of Be with $c/a = 1.568$.

K_1/η_1	Magnitude of shear s	Deformation matrix **S**	Re-indexation matrix **U**	Correspondence matrix **C**
$(\bar{1}012)$ $[10\bar{1}1]$	0.199339	$\begin{bmatrix} 0.925616 & -0.0429454 & 0.094877 \\ -0.0429454 & 0.975205 & 0.0547773 \\ -0.0777556 & -0.0448922 & 1.09918 \end{bmatrix}$	$\begin{bmatrix} -0.324384 & 0.390067 & -0.861756 \\ 0.390067 & -0.774795 & -0.497535 \\ -0.861756 & -0.497535 & 0.0991781 \end{bmatrix}$	$\begin{bmatrix} -0.25 & 0.433013 & -0.956633 \\ 0.433013 & -0.75 & -0.552312 \\ -0.784 & -0.452643 & 0 \end{bmatrix}$
$(10\bar{1}1)$ $[10\bar{1}\bar{2}]$	0.076817	$\begin{bmatrix} 1.02438 & 0.0140772 & 0.01555 \\ 0.0140772 & 1.00813 & 0.0089778 \\ -0.0509755 & -0.0294307 & 0.96749 \end{bmatrix}$	$\begin{bmatrix} 0.149382 & 0.663596 & 0.733024 \\ 0.663596 & -0.616873 & 0.423212 \\ 0.733024 & 0.423212 & -0.53251 \end{bmatrix}$	$\begin{bmatrix} 0.125 & 0.649519 & 0.717474 \\ 0.649519 & -0.625 & 0.414234 \\ 0.784 & 0.452643 & -0.5 \end{bmatrix}$
$(11\bar{2}2)$ $[11\bar{2}\bar{3}]$	0.194993	$\begin{bmatrix} 1.0221 & 0.0382792 & 0.0281894 \\ 0.0382792 & 1.0663 & 0.0488255 \\ -0.0693072 & -0.120044 & 0.911598 \end{bmatrix}$	$\begin{bmatrix} -0.644566 & 0.615629 & 0.453359 \\ 0.615629 & 0.0663015 & 0.785242 \\ 0.453359 & 0.785242 & -0.421735 \end{bmatrix}$	$\begin{bmatrix} -0.666667 & 0.57735 & 0.42517 \\ 0.57735 & 0 & 0.736416 \\ 0.522667 & 0.905285 & -0.333333 \end{bmatrix}$
$(11\bar{2}1)$ $[\bar{1}\bar{1}26]$	0.637755	$\begin{bmatrix} 0.953851 & -0.0799322 & -0.0294317 \\ -0.0799322 & 0.861553 & -0.0509772 \\ 0.289446 & 0.501335 & 1.1846 \end{bmatrix}$	$\begin{bmatrix} -0.546149 & 0.786093 & 0.289446 \\ 0.786093 & 0.361553 & 0.501335 \\ 0.289446 & 0.501335 & -0.815404 \end{bmatrix}$	$\begin{bmatrix} -0.5 & 0.866025 & 0.318878 \\ 0.866025 & 0.5 & 0.552312 \\ 0.0 & 0.0 & -1.0 \end{bmatrix}$

Table 3a
Transformation of parent slip systems to slip systems inside the twin in Mg $c/a = 1.624$, twinning mode $(\bar{1}\ 0\ 1\ 2)[1\ 0\ \bar{1}\ 1]$, twinning shear = 0.12891692.

	Parent slip system	Twin slip system
Basal slip systems	$(0001)[2\bar{1}\bar{1}0]$	$(\bar{1}010)[\bar{1}2\bar{1}\bar{3}]$
	$(0001)[\bar{1}2\bar{1}0]$	$(\bar{1}010)[\bar{1}\bar{2}10]$
	$(0001)[\bar{1}\bar{1}20]$	$(\bar{1}010)[\bar{1}\bar{2}\bar{1}3]$
Prismatic slip systems	$(10\bar{1}0)[\bar{1}2\bar{1}0]$	$(000\bar{1})[\bar{1}\bar{2}10]$
	$(0\bar{1}10)[2\bar{1}\bar{1}0]$	$(\bar{1}2\bar{1}2)[\bar{1}2\bar{1}\bar{3}]$
	$(\bar{1}100)[\bar{1}\bar{1}20]$	$(1\bar{2}12)[\bar{1}2\bar{1}3]$
Pyramidal⟨a⟩ slip systems	$(10\bar{1}1)[\bar{1}2\bar{1}0]$	$(\bar{1}014)[\bar{1}\bar{2}10]$
	$(0\bar{1}11)[2\bar{1}\bar{1}0]$	$(\bar{1}101)[\bar{1}2\bar{1}\bar{3}]$
	$(\bar{1}101)[\bar{1}\bar{1}20]$	$(0\bar{1}11)[\bar{1}2\bar{1}3]$
	$(\bar{1}011)[\bar{1}2\bar{1}0]$	$(\bar{1}014)[1\bar{2}10]$
	$(01\bar{1}1)[2\bar{1}\bar{1}0]$	$(0\bar{1}1\bar{1})[\bar{1}2\bar{1}\bar{3}]$
	$(1\bar{1}01)[11\bar{2}0]$	$(\bar{1}10\bar{1})[\bar{1}2\bar{1}\bar{3}]$
Pyramidal⟨c + a⟩ slip systems	$(10\bar{1}1)[\bar{1}\bar{1}23]$	$(\bar{1}014)[\bar{7}253]$
	$(10\bar{1}1)[\bar{2}113]$	$(\bar{1}014)[\bar{5}273]$
	$(0\bar{1}11)[11\bar{2}3]$	$(\bar{1}101)[\bar{5}\bar{2}73]$
	$(0\bar{1}11)[\bar{1}2\bar{1}3]$	$(\bar{1}101)[\bar{1}\bar{1}20]$
	$(\bar{1}101)[2\bar{1}\bar{1}3]$	$(0\bar{1}11)[\bar{7}253]$
	$(\bar{1}101)[\bar{1}\bar{2}13]$	$(0\bar{1}11)[\bar{2}110]$
	$(\bar{1}011)[2\bar{1}\bar{1}3]$	$(\bar{1}014)[\bar{7}253]$
	$(\bar{1}011)[11\bar{2}3]$	$(\bar{1}014)[\bar{5}273]$
	$(01\bar{1}1)[\bar{1}\bar{1}23]$	$(0\bar{1}1\bar{1})[\bar{7}253]$
	$(01\bar{1}1)[\bar{1}2\bar{1}3]$	$(0\bar{1}1\bar{1})[\bar{2}110]$
	$(1\bar{1}01)[\bar{2}113]$	$(\bar{1}10\bar{1})[\bar{5}\bar{2}73]$
	$(1\bar{1}01)[\bar{1}2\bar{1}3]$	$(\bar{1}10\bar{1})[\bar{1}\bar{1}20]$
K_1 / η_1	$(\bar{1}012)[10\bar{1}1]$	$(\bar{1}012)[\bar{1}01\bar{1}]$
K_2 / η_2	$(\bar{1}01\bar{2})[10\bar{1}\bar{1}]$	$(10\bar{1}2)[10\bar{1}\bar{1}]$

Table 3b
Transformation of parent slip systems to slip systems inside the twin in Mg $c/a = 1.624$, twinning mode $(1\ 0\ \bar{1}\ 1)[1\ 0\ \bar{1}\ \bar{2}]$, twinning shear = 0.13771653.

	Parent slip system	Twin slip system
Basal slip systems	$(0001)[2\bar{1}\bar{1}0]$	$(10\bar{1}\bar{1})[14\bar{5}6]$
	$(0001)[\bar{1}2\bar{1}0]$	$(10\bar{1}\bar{1})[1\bar{2}10]$
	$(0001)[\bar{1}\bar{1}20]$	$(10\bar{1}\bar{1})[\bar{5}41\bar{6}]$
Prismatic slip systems	$(10\bar{1}0)[\bar{1}2\bar{1}0]$	$(10\bar{1}3)[1\bar{2}10]$
	$(0\bar{1}10)[2\bar{1}\bar{1}0]$	$(\bar{3}4\bar{1}3)[14\bar{5}6]$
	$(\bar{1}100)[\bar{1}\bar{1}20]$	$(1\bar{4}\bar{3}3)[\bar{5}41\bar{6}]$
Pyramidal⟨a⟩ slip systems	$(10\bar{1}1)[\bar{1}2\bar{1}0]$	$(10\bar{1}1)[1\bar{2}10]$
	$(0\bar{1}11)[2\bar{1}\bar{1}0]$	$(\bar{1}4\bar{3}\bar{5})[14\bar{5}6]$
	$(\bar{1}101)[\bar{1}\bar{1}20]$	$(3\bar{4}1\bar{5})[\bar{5}41\bar{6}]$
	$(\bar{1}011)[\bar{1}2\bar{1}0]$	$(000\bar{1})[1\bar{2}10]$
	$(01\bar{1}1)[2\bar{1}\bar{1}0]$	$(\bar{5}4\bar{1}1)[14\bar{5}6]$
	$(1\bar{1}01)[11\bar{2}0]$	$(14\bar{5}1)[\bar{5}41\bar{6}]$
Pyramidal⟨c + a⟩ slip systems	$(10\bar{1}1)[\bar{1}\bar{1}23]$	$(10\bar{1}1)[11\bar{2}\bar{3}]$
	$(10\bar{1}1)[2\bar{1}\bar{1}3]$	$(10\bar{1}1)[2\bar{1}\bar{1}\bar{3}]$
	$(0\bar{1}11)[11\bar{2}3]$	$(\bar{1}4\bar{3}\bar{5})[7\bar{2}\bar{5}0]$
	$(0\bar{1}11)[\bar{1}2\bar{1}3]$	$(\bar{1}4\bar{3}\bar{5})[13\bar{8}\bar{5}6]$
	$(\bar{1}101)[2\bar{1}\bar{1}3]$	$(3\bar{4}1\bar{5})[5\bar{2}70]$
	$(\bar{1}101)[\bar{1}2\bar{1}3]$	$(3\bar{4}1\bar{5})[58\bar{1}\bar{3}6]$
	$(\bar{1}011)[2\bar{1}\bar{1}3]$	$(000\bar{1})[5\bar{2}70]$
	$(\bar{1}011)[11\bar{2}3]$	$(000\bar{1})[7\bar{2}\bar{5}0]$
	$(01\bar{1}1)[\bar{1}\bar{1}23]$	$(\bar{5}4\bar{1}1)[11\bar{2}\bar{3}]$
	$(01\bar{1}1)[\bar{1}2\bar{1}3]$	$(\bar{5}4\bar{1}1)[58\bar{1}\bar{3}6]$
	$(1\bar{1}01)[\bar{2}113]$	$(14\bar{5}1)[2\bar{1}\bar{1}\bar{3}]$
	$(1\bar{1}01)[\bar{1}2\bar{1}3]$	$(14\bar{5}1)[13\bar{8}\bar{5}6]$
K_1/η_1	$(10\bar{1}1)[10\bar{1}\bar{2}]$	$(10\bar{1}1)[\bar{1}012]$
K_2/η_2	$(10\bar{1}\bar{3})[30\bar{3}2]$	$(\bar{1}013)[30\bar{3}2]$

the twin and only two acquire higher index configuration, becoming $\{\bar{1}\ 0\ 1\ \bar{2}\}\langle\bar{1}\ 2\ \bar{1}\ 0\rangle_T$. Of the 12 pyramidal $\langle c + a\rangle$ slip systems, four preserve their type, four acquire higher index configuration becoming $\{\bar{1}\ 0\ 1\ \bar{2}\}\langle 2\ 2\ \bar{4}\ \bar{3}\rangle_T$, and the remaining four acquire lower index configuration becoming $\{0\ 1\ \bar{1}\ 0\}\langle 0\ 0\ 0\ 1\rangle_T$ and $\{1\ \bar{1}\ 0\ 0\}\langle 1\ \bar{1}\ 0\ \bar{1}\rangle_T$. The nature of the twinning products in Zr suggests then, that in certain cases tensile twinning in Zr may not necessary lead to hardening (Table 4b). As far as the author is aware there are at present no published experimental data to prove or disprove this concept. Some isolated micro-hardness measurements on $\{1\ 1\ \bar{2}\ 2\}$ compressive twins in Ti show, as expected, that these elements of the substructure are stronger than the surrounding matrix [19].

Geometrical considerations imply that the onset of twinning in hcp metals leads to production of qualitatively new defects in the twinned lattice; there are published data which confirm this. Paton and Backofen [20] reported high densities of previously unknown dislocations in the twinned material which were not present in the parent lattice; these were suspected of being either $\langle c\rangle$ or $\langle c + a\rangle$ sessile dislocations. Song and Gray [21] observed at least

Table 4a
Transformation of parent slip systems to slip systems inside the twin in Zr c/a = 1.594, twinning mode (1 1 $\bar{2}$ 2)[1 1 $\bar{2}$ $\bar{3}$], twinning shear = 0.226197.

	Parent slip system	Twin slip system
Basal slip systems	(0001)[2$\bar{1}\bar{1}$0]	(11$\bar{2}\bar{1}$)[$\bar{4}$5$\bar{1}$3]
	(0001)[$\bar{1}$2$\bar{1}$0]	(11$\bar{2}\bar{1}$)[5$\bar{4}\bar{1}$3]
	(0001)[$\bar{1}\bar{1}$20]	(11$\bar{2}\bar{1}$)[$\bar{1}\bar{1}$26]
Prismatic slip systems	(10$\bar{1}$0)[$\bar{1}$2$\bar{1}$0]	($\bar{1}$2$\bar{1}$4)[5$\bar{4}\bar{1}$3]
	(0$\bar{1}$10)[2$\bar{1}\bar{1}$0]	($\bar{2}\bar{1}\bar{1}$4)[$\bar{4}$5$\bar{1}$3]
	($\bar{1}$100)[$\bar{1}\bar{1}$20]	(1$\bar{1}$00)[$\bar{1}\bar{1}$26]
Pyramidal<a> slip systems	(10$\bar{1}$1)[$\bar{1}$2$\bar{1}$0]	(01$\bar{1}\bar{1}$)[5$\bar{4}\bar{1}$3]
	(0$\bar{1}$11)[2$\bar{1}\bar{1}$0]	($\bar{1}$2$\bar{1}$5)[$\bar{4}$5$\bar{1}$3]
	($\bar{1}$101)[$\bar{1}\bar{1}$20]	(4$\bar{2}\bar{2}$1)[$\bar{1}\bar{1}$26]
	($\bar{1}$011)[$\bar{1}$2$\bar{1}$0]	(2$\bar{1}\bar{1}$5)[5$\bar{4}\bar{1}$3]
	(01$\bar{1}\bar{1}$)[2$\bar{1}\bar{1}$0]	(10$\bar{1}\bar{1}$)[$\bar{4}$5$\bar{1}$3]
	(1$\bar{1}$01)[$\bar{1}$120]	($\bar{2}\bar{4}\bar{2}$1)[$\bar{1}\bar{1}$26]
Pyramidal<c+a> slip systems	(10$\bar{1}$1)[$\bar{1}\bar{1}$23]	(01$\bar{1}\bar{1}$)[11$\bar{2}$3]
	(10$\bar{1}$1)[$\bar{2}$113]	(01$\bar{1}\bar{1}$)[$\bar{8}\bar{1}\bar{7}$6]
	(0$\bar{1}$11)[11$\bar{2}$3]	($\bar{1}$2$\bar{1}$5)[55$\bar{1}\bar{0}$3]
	(0$\bar{1}$11)[$\bar{1}$2$\bar{1}$3]	($\bar{1}$2$\bar{1}$5)[10$\bar{1}$0]
	($\bar{1}$101)[2$\bar{1}\bar{1}$3]	(4$\bar{2}\bar{2}$1)[01$\bar{1}$0]
	($\bar{1}$101)[$\bar{1}$2$\bar{1}$3]	(4$\bar{2}\bar{2}$1)[$\bar{1}$8$\bar{7}\bar{6}$]
	($\bar{1}$011)[2$\bar{1}\bar{1}$3]	(2$\bar{1}\bar{1}$5)[01$\bar{1}$0]
	($\bar{1}$011)[11$\bar{2}$3]	(2$\bar{1}\bar{1}$5)[55$\bar{1}\bar{0}$3]
	(01$\bar{1}\bar{1}$)[$\bar{1}\bar{1}$23]	(10$\bar{1}\bar{1}$)[11$\bar{2}$3]
	(01$\bar{1}\bar{1}$)[$\bar{1}$2$\bar{1}$3]	(10$\bar{1}\bar{1}$)[$\bar{1}$8$\bar{7}\bar{6}$]
	(1$\bar{1}$01)[$\bar{2}$113]	($\bar{2}\bar{4}\bar{2}$1)[$\bar{8}\bar{1}\bar{7}$6]
	(1$\bar{1}$01)[$\bar{1}$2$\bar{1}$3]	($\bar{2}\bar{4}\bar{2}$1)[10$\bar{1}$0]
K_1/η_1	(11$\bar{2}\bar{2}$)[11$\bar{2}\bar{3}$]	(11$\bar{2}\bar{2}$)[$\bar{1}\bar{1}$23]
K_2/η_2	(11$\bar{2}\bar{4}$)[22$\bar{4}\bar{3}$]	($\bar{1}\bar{1}$24)[22$\bar{4}\bar{3}$]

Table 4b
Transformation of parent slip systems to slip systems inside the twin in Zr c/a = 1.594, twinning mode (1 1 $\bar{2}$ 1)[$\bar{1}$ $\bar{1}$ 2 6], twinning shear = 0.627353.

	Parent slip system	Twin slip system
Basal slip systems	(0001)[2$\bar{1}\bar{1}$0]	(000$\bar{1}$)[$\bar{1}$2$\bar{1}$0]
	(0001)[$\bar{1}$2$\bar{1}$0]	(000$\bar{1}$)[2$\bar{1}\bar{1}$0]
	(0001)[$\bar{1}\bar{1}$20]	(000$\bar{1}$)[$\bar{1}\bar{1}$20]
Prismatic slip systems	(10$\bar{1}$0)[$\bar{1}$2$\bar{1}$0]	(01$\bar{1}\bar{1}$)[2$\bar{1}\bar{1}$0]
	(0$\bar{1}$10)[2$\bar{1}\bar{1}$0]	($\bar{1}$01$\bar{1}$)[$\bar{1}$2$\bar{1}$0]
	($\bar{1}$100)[$\bar{1}\bar{1}$20]	(1$\bar{1}$00)[$\bar{1}\bar{1}$20]
Pyramidal<a> slip systems	(10$\bar{1}$1)[$\bar{1}$2$\bar{1}$0]	(01$\bar{1}$0)[2$\bar{1}\bar{1}$0]
	(0$\bar{1}$11)[2$\bar{1}\bar{1}$0]	($\bar{1}$01$\bar{2}$)[$\bar{1}$2$\bar{1}$0]
	($\bar{1}$101)[$\bar{1}\bar{1}$20]	(1$\bar{1}$0$\bar{1}$)[$\bar{1}\bar{1}$20]
	($\bar{1}$011)[$\bar{1}$2$\bar{1}$0]	(0$\bar{1}\bar{1}$2)[2$\bar{1}\bar{1}$0]
	(01$\bar{1}\bar{1}$)[2$\bar{1}\bar{1}$0]	(10$\bar{1}$0)[$\bar{1}$2$\bar{1}$0]
	(1$\bar{1}$01)[11$\bar{2}$0]	($\bar{1}$10$\bar{1}$)[11$\bar{2}$0]
Pyramidal<c+a> slip systems	(10$\bar{1}$1)[$\bar{1}\bar{1}$23]	(01$\bar{1}$0)[000$\bar{1}$]
	(10$\bar{1}$1)[$\bar{2}$113]	(01$\bar{1}$0)[2$\bar{1}\bar{1}$3]
	(0$\bar{1}$11)[11$\bar{2}$3]	($\bar{1}$01$\bar{2}$)[22$\bar{4}\bar{3}$]
	(0$\bar{1}$11)[$\bar{1}$2$\bar{1}$3]	($\bar{1}$01$\bar{2}$)[10$\bar{1}\bar{1}$]
	($\bar{1}$101)[2$\bar{1}\bar{1}$3]	(1$\bar{1}$0$\bar{1}$)[01$\bar{1}\bar{1}$]
	($\bar{1}$101)[$\bar{1}$2$\bar{1}$3]	(1$\bar{1}$0$\bar{1}$)[$\bar{1}$2$\bar{1}\bar{3}$]
	($\bar{1}$011)[2$\bar{1}\bar{1}$3]	(0$\bar{1}\bar{1}$2)[01$\bar{1}\bar{1}$]
	($\bar{1}$011)[11$\bar{2}$3]	(0$\bar{1}\bar{1}$2)[22$\bar{4}\bar{3}$]
	(01$\bar{1}\bar{1}$)[$\bar{1}\bar{1}$23]	(10$\bar{1}$0)[000$\bar{1}$]
	(01$\bar{1}\bar{1}$)[$\bar{1}$2$\bar{1}$3]	(10$\bar{1}$0)[$\bar{1}$2$\bar{1}\bar{3}$]
	(1$\bar{1}$01)[$\bar{2}$113]	($\bar{1}$10$\bar{1}$)[2$\bar{1}\bar{1}$3]
	(1$\bar{1}$01)[$\bar{1}$2$\bar{1}$3]	($\bar{1}$10$\bar{1}$)[10$\bar{1}\bar{1}$]
K_1/η_1	(11$\bar{2}\bar{1}$)[$\bar{1}\bar{1}$26]	(11$\bar{2}\bar{1}$)[11$\bar{2}$6]
K_2/η_2	(0001)[$\bar{1}\bar{1}$20]	(000$\bar{1}$)[$\bar{1}\bar{1}$20]

two kinds of defects unique to deformations twins in Zr and Ti, sessile [0 0 0 1] dislocations in {1 0 $\bar{1}$ 2} tensile twins produced as a result of trapping matrix $\langle a \rangle$ dislocations, and a high density of stacking faults terminated by partial dislocations of sessile character with considerably smaller Burgers vector than that of partial dislocations formed in these metals. The presence of these defects was confirmed in recent TEM studies of deformed Zr by Bhattacharya and co-workers [9], who argued that transformed dislocations increase resistance to dislocation propagation in the twin lattice and at least partially contribute to the macroscopic hardening of the material.

Depending upon the character of the parent defect and its transformed product, our studies of fcc materials have defined five different types of transformations of lattice defects by twinning [6]. These included transformations of glissile dislocations in the matrix to sessile dislocations in the twin, sessile dislocations in the matrix to glissile products in the twin, glissile to glissile and sessile to sessile transformations, and transformations of three-dimensional defects. It was shown that the nature of dislocations in the twin lattice is predicted by the correspondence matrix. The process of incorporating dislocations into the twin lattice can be described by geometrical modeling techniques, provided conditions of a true generating node can be satisfied.

On the other hand, atomistic modeling of interactions of twinning dislocations with stacking fault tetrahedra in copper suggest that these interactions are governed by the energy of the system and the nature of the resulting defects might be different from those predicted by the geometrical considerations and the correspondence matrix alone [22,23]. Also, electrical resistivity studies of deformed copper show that a twinned substructure acquires an unusually high density of recoverable defects which anneal out at relatively low temperatures, indicating that heavy refinement of pre-existing defects occurs as a result of the interactions of twinning dislocations with these elements of the dislocation substructure [24]. However, many dislocations in fcc crystals transform as predicted by operation of the correspondence matrix [4,6,7]. It is apparent that there is still much to learn about the details of mechanical twinning in hcp metals and that more systematic work, both experimental and theoretical, is needed to better understand the processes and the structures involved.

5. Summary

We have outlined a method for obtaining the deformation, re-indexation, and correspondence matrices for different modes of compound twinning in hcp crystal structures and have provided explicit forms of these matrices. The method was used to analyze the correspondence of slip modes in the parent and twinned structures of Mg and Zr. Possible consequences of the lattice correspondence on the hardening of deformation twins in these metals were discussed. The method is applicable to other

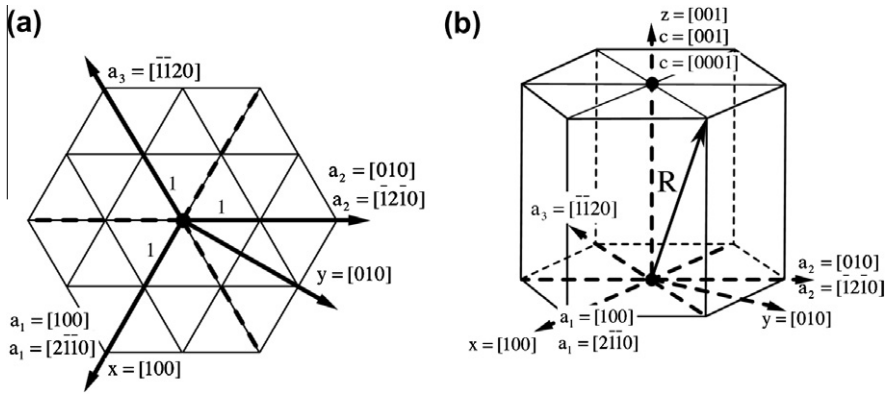

Fig. A1. Relation between hexagonal $\mathbf{a}_1$, $\mathbf{a}_2$, $\mathbf{a}_3$, $\mathbf{c}$, rhombohedral $\mathbf{a}_1$, $\mathbf{a}_2$, $\mathbf{c}$, and orthogonal **x, y, z** coordinate axis system in planar (a) and perspective view (b). Components of the vector R in (b) defined with respect to hexagonal, rhombohedral and orthonormal basis vectors are: $R = [1,1,-2,1]$, $R = [1,1,1]$ and $R = \left[1, \sqrt{3}, \frac{2c}{a}\right]$ respectively.

studies of lattice transformations due to twinning in hcp materials.

Acknowledgement

Stimulating discussions with Dr. Carlos Tome of Los Alamos National Laboratory are gratefully acknowledged.

Appendix A. Transformation of hexagonal indices to orthonormal coordinate system

Different relationships between three and four-index notation may be derived for hexagonal crystal system (see e.g. Ref. [25]). The procedure described below involves forward and reverse transformation of indices of crystallographic planes and directions form hexagonal to rhombohedral to orthogonal coordinate systems.

Arbitrary direction **R** with Miller–Bravais indices $[u\ v\ t\ w]$ in hexagonal crystal system defined with respect to four basis vectors $\mathbf{a_1}$, $\mathbf{a_2}$, $\mathbf{a_3}$, $\mathbf{c}$ can be expressed in a rhombohedral system defined with three basis vectors $\mathbf{a_1}$, $\mathbf{a_2}$, $\mathbf{c}$ using three-index Miller notation $[U\ V\ W]$ such that:

$$\mathbf{R} = u\mathbf{a_1} + v\mathbf{a_2} + t\mathbf{a_3} + w\mathbf{c}$$

and

$$\mathbf{R} = U\mathbf{a_1} + V\mathbf{a_2} + W\mathbf{c}$$

The hexagonal $[u\ v\ t\ w]$ and rhombohedral $[U\ V\ W]$ indices satisfy following transformation relations between these axes systems [26]:

$$U = u - t \quad V = v - t \quad W = w$$
$$u = \frac{1}{3}(2U - V) \quad v = \frac{1}{3}(2V - U) \quad t = -(u + v) \quad w = W \tag{A1}$$

The Miller–Bravais indices $(h\ k\ i\ l)$ of a crystallographic plane **n** in hexagonal crystal system and Miller indices $(H\ K\ L)$ of the same plane in rhombohedral axis system are expressed as components of a reciprocal vector defined with respect to the four reciprocal basis vectors of hexagonal crystal system or three reciprocal basis vectors of romboherdral lattice such that:

$$\mathbf{n} \equiv \mathbf{g_{hkil}} = h\mathbf{a_1^*} + k\mathbf{a_2^*} + i\mathbf{a_3^*} + l\mathbf{c^*}$$

and

$$\mathbf{n} \equiv \mathbf{g_{HKL}} = H\mathbf{A_1^*} + K\mathbf{A_2^*} + L\mathbf{C^*}$$

Here, $\mathbf{a_1^*}$, $\mathbf{a_2^*}$, $\mathbf{a_3^*}$ and $\mathbf{c^*}$ are reciprocal basis vectors for hexagonal system $\mathbf{a_1}$, $\mathbf{a_2}$, $\mathbf{a_3}$, $\mathbf{c}$ and $\mathbf{A_1^*}$, $\mathbf{A_2^*}$, $\mathbf{C^*}$ are reciprocal basis vectors for rhombohedral system $\mathbf{a_1}$, $\mathbf{a_2}$, $\mathbf{c}$. The direct and reciprocal basis vectors in hexagonal and rhombohedral axis system, satisfy reciprocity conditions: $a_i \cdot a_j^* = \delta_{ij},\ i,j = 1,4$ and $a_i \cdot A_j^* = \delta_{ij},\ i,j = 1,3$, where δ_{ij} is 4×4 or 3×3 Kronecker delta in hexagonal and rhombohedral systems, respectively.

The Miller–Bravais and Miller indices of a plane in hexagonal and rhombohedral axis system satisfy following relations [26]:

$$\begin{aligned} &H = h \quad K = k \quad L = l \\ &h = H \quad k = K \quad i = -(h + k) \quad l = L \end{aligned} \tag{A2}$$

If the vector **R** belongs to the plane **n**, than in any reference system, the plane and the vector must satisfy orthogonality conditions, i.e. $\mathbf{R} \cdot \mathbf{n} = 0$ or $uh + vk + ti + wl = 0$ and $UH + VK + WL = 0$.

The transformation from the rhombohedral $\mathbf{a_1}$, $\mathbf{a_2}$, $\mathbf{c}$ to orthonormal **x**, **y**, **z** coordinate system in which subsequent calculations are carried out (Fig. A1), is done by means of a transformation matrix **A**:

$$\mathbf{A} = \begin{pmatrix} 1 & -\frac{1}{2} & 0 \\ 0 & \frac{\sqrt{3}}{2} & 0 \\ 0 & 0 & \frac{c}{a} \end{pmatrix}$$

where c and a are lattice parameters of the hexagonal lattice.

Indices of a vector $\mathbf{R}_{[\mathbf{xyz}]} \equiv [x\ y\ z]$ in orthonormal **x**, **y**, **z** coordinate system are obtained by coordinate transformation of indices of a vector $\mathbf{R}_{[\mathbf{UVW}]} \equiv [U\ V\ W]$ in rhombohedral system such that:

$$\mathbf{R}_{[\mathbf{xyz}]} = \mathbf{A}\ \mathbf{R}_{[\mathbf{UVW}]}$$

A is a transformation matrix from rhombohedral to orthonormal system, and $\mathbf{R}_{[\mathbf{xyz}]}$ and $\mathbf{R}_{[\mathbf{UVW}]}$ are column vectors.

Similarly, the indices of a plane $\mathbf{n}_{[\mathbf{xyz}]} \equiv (x\ y\ z)$ in orthonormal **x**, **y**, **z** coordinate system are obtained by coordinate transformation of indices of plane $\mathbf{n}_{[\mathbf{HKL}]} \equiv (H\ K\ L)$ such that:

$$\mathbf{n}_{(\mathbf{xyz})} = \mathbf{n}_{(\mathbf{HKL})}\ \mathbf{A}^{-1}$$

$\mathbf{A}^{-1}$ is the inverse of the matrix **A**, whereas $\mathbf{n}_{(\mathbf{xyz})}$ and $\mathbf{n}_{(\mathbf{HKL})}$ are row vectors.

After transformation to **x**, **y**, **z** system, the vector $\mathbf{R}_{[\mathbf{xyz}]}$ and the plane $\mathbf{n}_{(\mathbf{xyz})}$ must satisfy orthogonality conditions $\mathbf{R}_{[\mathbf{xyz}]} \cdot \mathbf{n}_{(\mathbf{xyz})} = 0$.

The reversible transformations of a vector and a plane from orthonormal to rhombohedral system are done as follows:

$$\mathbf{R}_{[\mathbf{UVW}]} = \mathbf{A}^{-1}\ \mathbf{R}_{[\mathbf{xyz}]}$$
$$\mathbf{n}_{(\mathbf{HKL})} = \mathbf{n}_{(\mathbf{xyz})}\ \mathbf{A}$$

Transformation from rhombohedral to hexagonal system is done by means of Eqs. (A1) and (A2), as discussed above.

Appendix B. Calculation of an angle between vectors or planes in hexagonal lattice

The direction given by Miller–Bravais indices $[u\ v\ t\ w]$ is the Cartesian four-dimensional vector **v** with components $\mathbf{v} = [u, v, t, \lambda w]$ [27]. Similarly, a crystallographic plane given by Miller–Bravais indices $(h\ k\ i\ l)$ is the Cartesian four-dimensional vector **p** with components $\mathbf{p} = [u,\ v,\ t,\ w/\lambda]$, where $\lambda = (c/a)(2/3)^{1/2}$, c and a are lattice parameters of hexagonal unit cell. The angle α between two of these four-dimensional vectors is given by the standard formula [27]:

$$\cos\alpha = \frac{v_1 \cdot v_2}{|v_1||v_2|} \quad \text{or} \quad \cos\alpha = \frac{p_1 \cdot p_2}{|p_1||p_2|}$$

where $v_1 \cdot v_2$ and $p_1 \cdot p_2$ are dot products of v_1, v_2 and p_1, p_2 vectors and $|v_1|$, $|v_2|$, $|p_1|$, $|p_2|$ are their lengths respectively.

References

[1] Kadiri HEl, Oppedal AL. J Mech Phys Solids 2010;58:613.
[2] Christian JW. The theory of transformations of metals and alloys. Oxford: Pergamon Press; 1965.
[3] Bevis M, Crocker AG. Proc R Soc Lond A: Math Phys Sci 1968;A304:123.
[4] Basinski ZS, Szczerba MS, Niewczas M, Embury JD, Basinski SJ. Revue de Métallurgie 1997;94:1037.
[5] Szczerba MS. Transformations of dislocations during twinning in cubic crystals. Krakow: Wydawnictwa AGH; 1996.
[6] Niewczas M. Dislocations and twinning in face centered cubic crystals. In: Nabarro FRN, Hirth JP, editors. Dislocations in solids. Oxford: Elsevier Science; 2007.
[7] Szczerba MS, Tokarski T, Perek M. Arch Metall Mater 2007;52:193.
[8] Chiu YL, Gregoriy F, Inuiz H, Veyssiere P. Philos Mag 2004;84:3235.
[9] Bhattacharyya D, Cerreta EK, McCabe R, Niewczas M, Gray III GT, Misra A, et al. Acta Mater 2009;57:305.
[10] Kelly A, Groves GW. Crystallography and crystal defects. London: Longman Group Limited; 1970.
[11] Bevis M, Crocker AG. Proc R Soc Lond A: Math Phys Sci 1969;A313:509.
[12] Partridge PG. Metall Rev 1967;12:169.
[13] Christian JW, Mahajan S. Prog Mater Sci 1995;39:1.
[14] Bilby BA, Crocker AG. Proc R Soc Lond A: Math Phys Sci 1965;A288:240.
[15] Yoo M. Metall Trans 1981;12A:409.
[16] Rosenbaum HS. Nonbasal slip in h.c.p. metals and its relation to mechanical twinning. In: Reed-Hill RE, Hirth JP, Rogers HC, editors. Deformation twinning. New York: Gordon and Breach Science Publishers; 1964.
[17] Chin GY, Thurston RN, Nesbitt EA. Trans Metall Soc AIME 1966;236:69.
[18] Roters F, Eisenlohr P, Hantcherli L, Tjahjanto DD, Bieler TR, Raabe D. Acta Mater 2010;58:1152.
[19] Salem AA, Kalidindi SR, Doherty RD, Semiatin SL. Metall Mater Trans 2006;37A:259.
[20] Paton NE, Backofen WA. Metall Trans 1970;1:2839.
[21] Song SG, Gray GT. Acta Metall Mater 1995;43:2339.
[22] Niewczas M, Hoagland RG. Philos Mag 2009;89:623.
[23] Niewczas M, Hoagland RG. Philos Mag 2009;89:727.
[24] Niewczas M, Basinski ZS, Basinski SJ, Embury JD. Philos Mag 2001;A81:1121.
[25] Hofmann DC, Lubarda VA. J Appl Crystallogr 2003;36:23.
[26] Barrett CS. Structure of metals: crystallographic methods, principles and data. New York: McGraw-Hill; 1952.
[27] Frank FC. Acta Crystallogr 1965;18:862.